ABRASIVE JET MACHINING FOR EDGE GENERATION

Matthew W. Chastagner and Albert J. Shih
Mechanical Engineering
University of Michigan
Ann Arbor, Michigan

KEYWORDS

Abrasive Jet Machining, Edge Finishing, Edge Generation, Erosion Wear

ABSTRACT

The edge with a consistent and precise shape is important for highly stressed mechanical components. This study investigates the generation, measurement, and definition of edges. Abrasive jet machining, a flexible process ideal for difficult-to-reach areas, is applied for edge generation. A conoscopy laser with small, 25 μm spot size is scanned across the edge for measurement. A B-spline curve is applied to fit the edge profile by an optimization method. Silicon carbide media, 50 μm average size, was used to erode a 90º edge on a workpiece of Inconel 718. Effects of blasting time, stand off distance between edge and nozzle, and orientation of a nozzle are studied. It is found that the edge radius is limited to below 0.15 mm using abrasive jet machining. Under long blasting durations, the edge radius does not change, but collateral damage around the edge is significant. Long standoff distances and high angles of blasting are beneficial in reducing the level of collateral damage. Edge radius is commonly used as the only parameter to quantitatively describe the edge profile. This study demonstrates that a B-spline can provide a better fit and geometrical description of the edge profile.

INTRODUCTION

Abrasive jet machining (AJM), also called abrasive micro blasting, is a manufacturing process that utilizes a high-pressure air stream carrying small particles to impinge the workpiece surface for material removal and shape generation. The removal occurs due to the erosive action of the particles striking the workpiece surface. AJM has limited material removal capability and is typically used as a finishing process (Gillespie 1999).

AJM is advantageous in two aspects. First, it has a high degree of flexibility. The abrasive media can be carried by a flexible hose to reach internal, difficult-to-reach regions. Second, AJM has localized force and less heat generation than traditional machining processes. In this study, AJM is investigated to generate a desired edge shape.

In highly stressed mechanical components, such as the turbine blades and rotors in aircraft engines it is important to avoid sharp edges, which can lead to cracks and premature part failure due to localized stress concentrations.

The technical challenges are the definition, measurement, and generation of edges with the desired shape. In difficult-to-reach edges, for example, at the intersection of holes inside the part, the generation and measurement of the edges are particularly challenging due to the geometrical constraints for limited tooling access. AJM, abrasive flow machining and turbo abrasive machining are all suitable for internal edge generation because of their ability to enter small holes and reach the internal edges (Gillespie 1999). The investigation into the use of AJM was undertaken since it can be applied directly to a single controlled location.

A variety of applications of AJM have been studied. Balasubramaniam et al. (1999, 2000) investigated using AJM to remove burrs at the intersection of cross-drilled holes on stainless steel, while also examining the subsequent edge radius. Lemaster et al. (2005) and Qu et al. (2005) have studied the use of AJM as a surface finishing process on wood and WC-Co composite, respectively. Others have examined the AJM process for glass etching and grooving in micro-systems parts (Park et al. 2004) and flat panel displays (Slikkerveer et al. 2000). Canby (2003) has reported AJM for removing burrs on very small holes in aircraft turbine blades. Balasubramaniam et al. (2000) has proposed a mathematical relationship for edge radius definition when using AJM on a blunt surface. However, this method does not take into account the edge radius created on a predefined sharp edge. Therefore, the investigation into the definition of an AJM generated edge has become one of the goals of this research. Another goal of this study is to develop the optical non-contact conoscopy laser measurement with a small, 25 μm, focal point spot size to quantify the shape of the edge after AJM under different processing conditions.

In the cutting tool industry, the shape of the edge is important for tool performance. The radius and waterfall shape are two commonly used features to define an edge (Shaffer 1999). However, the mathematical description of an edge has not been studied extensively. Using high resolution edge measurement, such as the conoscopy laser used in this study, can give a more detailed quantitative analysis of the edge. There is a need for a more precise definition of edge than just a radius. In this study, a mathematical model based on B-spline is investigated to provide a better fit to the measured edge profile. The level of fitness is quantified using an error index.

In this paper, the experimental setup of the AJM machine, blasting media, sample preparation, and laser edge measurement are first introduced. Effects of three key process parameters, the time of blasting, the stand off distance, and the angle of impingement, on the edge radius and collateral damage around the created edge are examined. Finally, the mathematical analysis of edge profile is studied.

EXPERIMENTAL SETUP

The AJM setup, edge measurement, experimental procedure, and edge profile analysis are discussed in the following sections.

AJM Machine Setup

The AJM machine is a Comco micro blaster, Model MB1000, in combination with a collector (Comco WS2200-1) for removing the spent media. This machine has an oscillating mechanical valve to meter the media into the air stream (Weightman 1970). This method is more complicated than using a venturi to draw the particles into a mixing chamber (Lemaster et al. 2005). The Comco machine design has the advantage of metering a small and precise amount of micro-size media for AJM. The mixture of media and airflow is then directed to a nozzle where it exits towards the part, as shown in Figure 1(A).

This AJM machine has an internal timer, allowing for the duration of the blast to be controlled precisely. A special fixture was designed and built to orient the nozzle and workpiece, which is defined by two parameters: the distance from the edge to the center of the nozzle and the angle between the nozzle and the edge, denoted as l and α in Figure 1(A), respectively. This fixture consisted of a toolmakers vise with an attachment for holding the nozzle perpendicular to the vise, as shown in Figure 1(B). Special machined jaw faces were made for the vice to hold the sample at the correct position. For tests in which the nozzle angle relative to the sample needed to be changed, angled inserts were used to orient the workpiece without moving the nozzle.

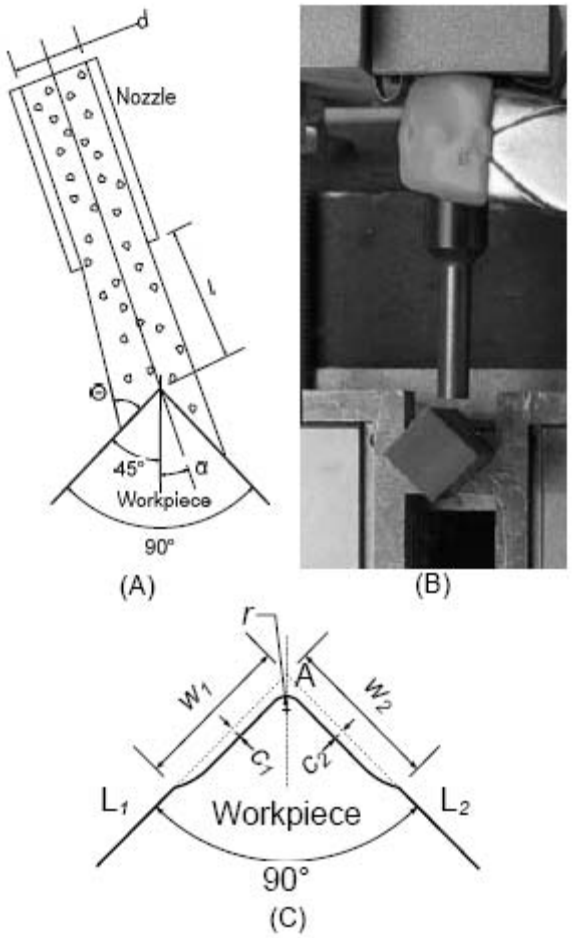

FIGURE 1. (A) CONFIGURATION OF THE SETUP AND KEY PARAMETERS, (B) PICTURE OF THE NOZZLE AND WORKPIECE, AND (C) WORKPIECE EDGE AFTER BLASTING WITH KEY GEOMETRICAL PARAMETERS.

The nozzle is made of tungsten carbide and has a round inner diameter, marked as *d* in Figure 1(A). In this study, *d* is 1.5 mm. Silicon carbide (SiC) media with a 50 µm average size is used as the blasting media. According to the guideline of the AJM machine builder, the nozzle inner diameter needs to be 20 times larger than the average media size. The SiC was selected due to its high hardness (2700 Knoop or 9+ Mohr hardness), in combination with its sharp blocky shape. This allows for effective erosion wear of the Inconel workpiece. Figure 2 shows the scanning electron microscope (SEM) (Philips XL30) micrographs of the shape and the size of the SiC media.

The angle of the edge investigated in this study is 90º. A wire electrical discharge machine (Brother HS-5100) was used to cut the Inconel 718 workpiece to create the sharp edge. Dimensions of the sample, as shown in Figure 1(B), were 6.40 mm x 6.40 mm x 20.0 mm. After AJM, the edge is eroded, to produce a rounded tip and collateral damage is present on both sides of the edge. As shown in Figure 1(C), the edge radius is marked by *r*, the width and depth of the collateral damage are denoted as w_1 and c_1 on the left side (close to the nozzle) and w_2 and c_2 on the right side (away from the nozzle). These parameters are applied to quantify the edge after AJM.

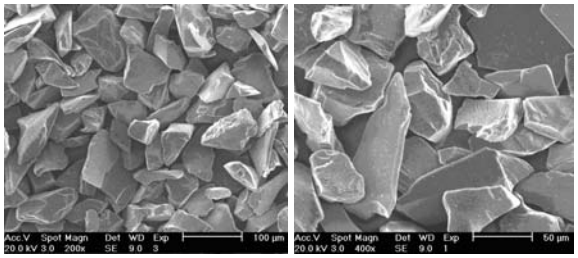

FIGURE 2. SEM MICROGRAPHS OF SiC MEDIA.

Edge Measurements

Figure 3(A) shows the setup to measure the edge profile using a conoscopy laser sensor (Optimet Smart ConoProbe #25). This sensor was chosen because it: (1) has a small, 25 µm focal point, (2) is precise with sub-µm accuracy, and (3) allows for a high incidence angle, up to 80º, in measurement. A computer-controlled stage, made by Aerotech™, is applied to move the sensor relative to the workpiece.

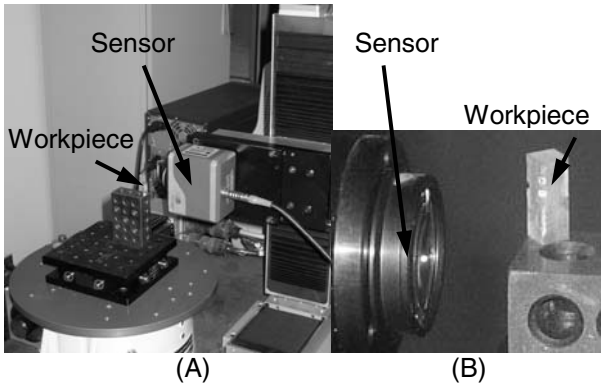

FIGURE 3. SETUP FOR THE EDGE PROFILE LASER MEASUREMENT.

The close-up view of the workpiece and sensor is shown in Figure 3(B). A line scan, with

a scanning speed of 100 mm/min and 3000 data points per second sampling frequency, resulted in about 8000 data points per edge. This line scan was applied across the edge.

Experimental Procedure

This research studies the effect of three key process parameters: l, α, and the time of blasting, t. The input air pressure to the nozzle was set at 552 kPa. Three sets of experiments, marked as Exps. I, II, and III, were performed.

- Exp. I maintained l = 0 mm and α = 0º, while t was varied from 0 to 15 in 1 s increments. Another test was conducted under the same conditions with t = 30 s. This experiment studies the effect of time of blasting.
- Exp. II investigates the effect of distance between nozzle and edge tip. The value of l was varied from 0 to 5 in 1 mm steps, while t = 7 s and α = 0º.
- Exp. III studies the effect of angle α, which was varied from 0º to 30º in 5º increments (with l = 0 mm and t = 7 s).

Three repeated tests were conducted for every test condition. All tests eroded a spot on the edge, as illustrated by spots on the workpiece edge in Figure 3(B). In production, the nozzle is expected to move along the edge to generate the desired edge radius. The spot test in this study is the first step in understanding the magnitude of the edge radius and collateral damage in AJM.

Edge Profile Analysis

The measured edge profile is recorded by the x-y cloud of data points and needs to be analyzed to determine the edge radius and level of collateral damage. To determine the edge radius, two boundary points are first identified to define the range for curve fitting an arc. A least-squares curve fitting method was utilized to fit an arc to all of the data points between two boundary points, thus finding the edge radius.

To determine the collateral damage, the straight side lines unaffected by AJM, marked as L_1 and L_2 in Figure 1(C), are first identified. These two lines intersect as a point, A. Two other control points are identified on the side line to determine the distances w_1 and w_2, respectively, from point A. The maximum distance from points in the collateral damaged region to L_1 and L_2 are searched to find c_1 and c_2, respectively.

RESULTS

SEM Micrographs of Edges After AJM

SEM micrographs of an AJM machined edge in Exp. I with t = 15 s are shown in Figure 4(A). A close-up view of the edge and the depth of collateral damage are shown in Figure 4(B). The number 1 is placed on the side with w_1 and c_1, i.e., the side close to the nozzle. The dashed line marks the edge profile measurement trace using the conoscopy laser. The collateral damage is obvious. Quantitative values of collateral damage will be discussed in the following section (Exp. I). Figure 4(C) shows the less obvious collateral damage in the Exp. II test with l = 5 mm, t = 7 s, and α = 0º.

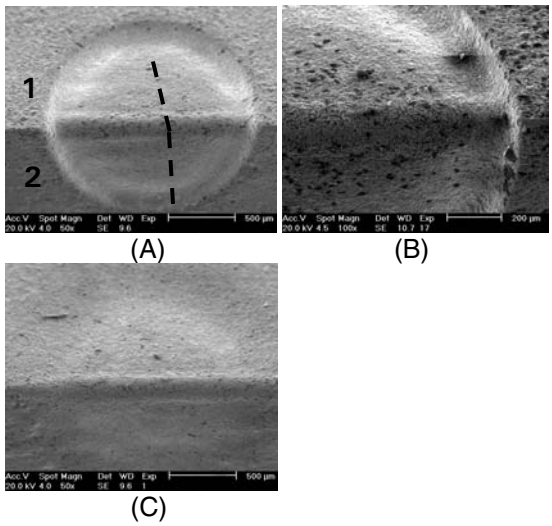

FIGURE 4. SEM MICROGRAPHS OF THE AJM REGION AND EDGES (A) EXP. I, 15 S, (B) CLOSE-UP VIEW OF (A), AND (C) EXP. II WITH 5 MM STANDOFF DISTANCE.

Exp. I. Effect of Blasting Time

Figure 5 shows results of r, c_1, c_2, w_1 and w_2 for the 16 tests in Exp. I. The error bars indicate the deviation of the three repeated tests from the average value. The edge radius of 0.022 mm at t = 0 represents the initial edge radius after wire EDM. The edge radius increases rapidly in the beginning of blasting to 0.07, 0.08, 0.09, and 0.10 mm after 1, 2, 3, and 4 s of blasting, respectively. As the edge takes its shape after 4 s, the edge radius increases very slowly from 0.12 to 0.13 mm. The long, 30 s blasting time produces a 0.14 mm edge radius, which is only

slightly increased from the 15 s value. This indicates that the edge radius in AJM is determined in the initial stage. This immediate steady state erosion has also been observed in steel (Tilly 1969). In Exps. II and III, 7 s has been selected as the time of blasting because of the steady-state nature of the edge radius generation.

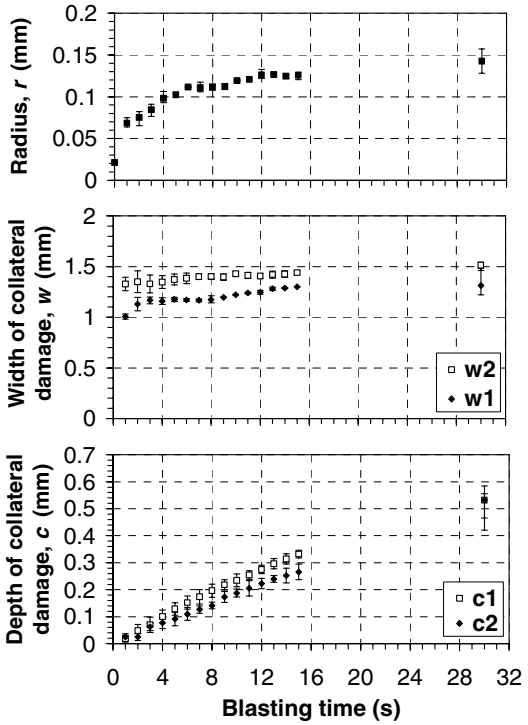

FIGURE 5. EFFECTS OF BLASTING TIME ON EDGE RADIUS AND DEPTH AND WIDTH OF COLLATERAL DAMAGE (EXP. I RESULTS).

The width of collateral damage, w_1 and w_2, ranges between 1.2 to 1.4 mm after 2 s of blasting. Blasting time does not change the width of collateral damage significantly after the first 2 s. Since $\alpha = 0^{\circ}$, w_1 and w_2 shall be close to each other. However, the difference between w_1 and w_2 indicates that an alignment error exists. It is difficult to setup the exact $\alpha = 0^{\circ}$ and such discrepancy is unavoidable.

Unlike the results of r, w_1, and w_2, the depth of collateral damage increases steadily and linearly with respect to time. After 15 s of blasting, c_1 was 0.33 mm, while c_2 was 0.26 mm. This linear trend extends to the 30 s long blasting time, which produces collateral damage about 0.5 mm deep. On average, each second of blasting erodes about 17 μm of material.

In conclusion, the Exp. I results in Figure 5 show that most of the AJM edge generation is taking place within the first 4 s, and after this, extended blasting times only cause a gradual increase of the depth and essentially no change in the width of the collateral damage.

Exp. II: Effect of Standoff Distance

Figure 6 shows the results of r, c_1, c_2, w_1 and w_2 for the 6 tests in Exp. II with l varying from 0 to 5 mm, while keeping t = 7 s and $\alpha = 0^{\circ}$. The edge radius remains about the same, 0.11 mm, independent of l. The collateral damage width has a slight increasing trend, but remains in the 1.3 to 1.5 mm range. The depth of collateral damage shows a steady trend of decreasing, from about 0.15 mm to 0.1 mm. The highest stand off distance (l = 5 mm), with the resulting smallest depth of collateral damage, corresponds to the SEM micrograph of the edge shown in Figure 4(C).

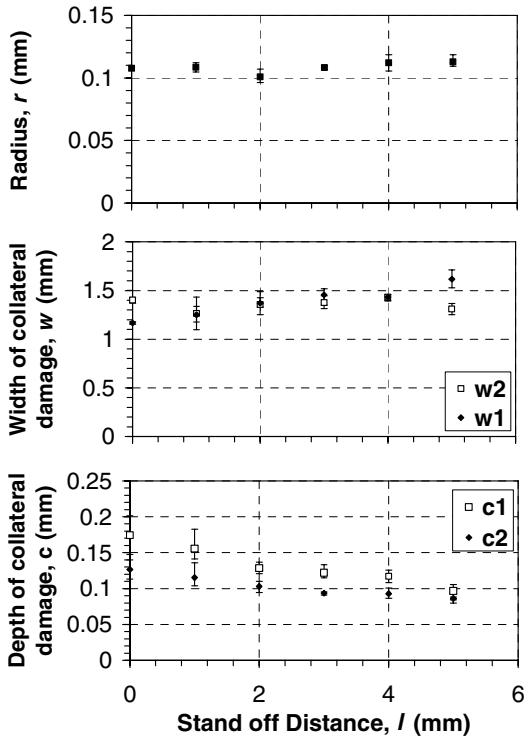

FIGURE 6. EFFECTS OF NOZZLE STAND OFF DISTANCE ON EDGE RADIUS AND DEPTH AND WIDTH OF COLLATERAL DAMAGE (EXP. II RESULTS).

Results in Exp. II point to a strategy of moving the nozzle tip away from edge to create the

same level of edge radius while reducing the depth of collateral damage.

Exp. III: Effect of Angle

Figure 7 shows the results of r, c_1, c_2, w_1 and w_2 for the 7 tests in Exp. III with α varying from 0° to 30°, while keeping t = 7 s and l = 0 mm. The edge radius remains within the 0.1 to 0.12 mm range and does not vary significantly with respect to the angle α.

The nozzle orientation has a significant impact on w_1 and w_2. As the angle α is stepped up from 0° to 30°, on the side close to the nozzle, w_1 decreases and, on the side away from the nozzle, w_2 increases. This is caused by the angle of impingement θ, as illustrated in Figure 1(A), of the particles impinging the surface.

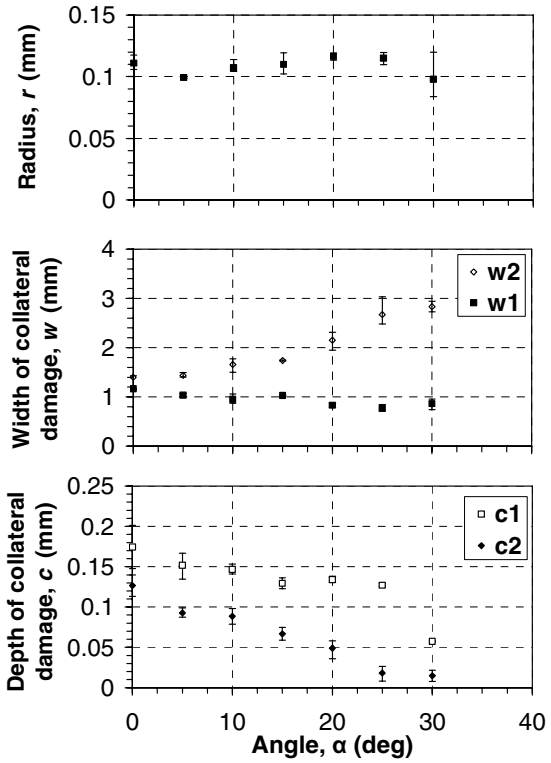

FIGURE 7. EFFECTS OF NOZZLE ORIENTATION ANGLE ON EDGE RADIUS AND DEPTH AND WIDTH OF COLLATERAL DAMAGE (EXP. III RESULTS).

Erosion wear is the mechanism for material removal in AJM. The angle of impingement affects the material removal rate significantly. For brittle materials, the maximum material removal rate occurs when the angle of impingement is about 90°, i.e., the particle velocity vector is perpendicular to the surface. On the contrary, for ductile materials, which include the Inconel 718 used in this study, the shallow angle of impingement will result in high material removal rate (Cousens and Hutchings 1983; Williams 1994). As shown in Figure 1(A), the area away from the nozzle has a shallow angle of impingement and will result in more material removal.

The erosion process for ductile material can be characterized by either a dentation-type, ploughing type or cutting type event (Morrison 1986). The dentation-type event only serves to move material, as it does not cut. Ploughing and cutting are the primary reason for the material removal. This removal occurs as the particle strikes the material, causing small platelets of material to be extracted from the surface and expelled. If the platelet is not fully removed, subsequent particles striking the surface will cause the platelet to finally become detached. This platelet removal process requires large shear deformations coupled with heat increase and very high strain rates (Shewmon 1981).

The angle α also has a significant effect on the depth of collateral damage. Both c_1 and c_2 show a trend of decreasing at high α. This is a pleasantly surprising observation. It can be explained by the angle of impingement. In the region close to the nozzle, the angle of impingement is close to 90° and the material removal rate is low because the work-material is ductile. In the region away from the nozzle, the angle of impingement is shallow; it can increase the width of collateral damage (w_2) but does not have enough speed and energy to create significant material removal.

Exps. II and III results show that it is possible to strategize the l and α to reduce collateral damage in AJM for edge generation.

ANALYSIS OF EDGE PROFILE

Various edge profiles are generated in AJM. Figure 8 illustrates the close-up view of seven edge profiles generated in Exp. III. The horizontal axis is the stage traverse distance and the vertical axis is the sensor measured distance. The profile shown in Figure 8 has been translated to make the lowest point in the sensor measurement equivalent to 0 in both the stage traversed and sensor measured distances.

The test profile of α = 10º in Exp. III is selected for further analysis. Two control points are selected to define the curve section for analysis. This section, marked in Figure 8, is rotated and re-oriented, as shown in Figure 9. Two curve fitting methods, a least-squares fitting of a circular arc and B-spline fit, are utilized to mathematically describe this edge profile.

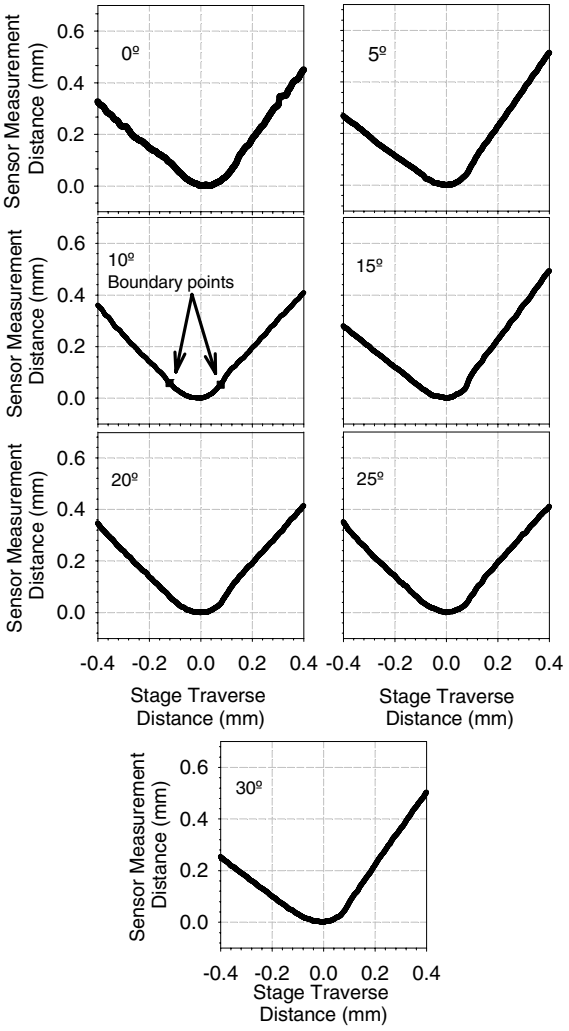

FIGURE 8. MEASURED EDGE PROFILE OF SEVEN TESTS IN EXP. III.

The result of fitting a circular arc to the edge profile is the edge radius. This single parameter fitting is not precise, as illustrated by the arc in Figure 9. An error index, *e*, is defined to quantify the level of accuracy in the curve fitting.

$$e = \sqrt{\sum_{i=1}^{N} (x_i^m - x_i^p)^2 \Big/ N}$$

where N is the number of sample points selected on the edge profile, x_i^m and x_i^p are the measured and curve fit predicted points of edge profile, respectively.

The B-spline curve has the freedom to select two control points to fit the edge profile. The B-spline is optimized using Matlab® to find the locations of control points, while minimizing the error index *e*. The circular arc and B-spline in Figure 9 have *e* = 1.6 and 4.4 μm, respectively. The B-spline has a better fit, which can also be recognized in Figure 9. One of the advantages of using circular arc is the result of a simple, single value for the edge representation and comparison. It remains as a technical challenge on how to better represent the B-spline curves.

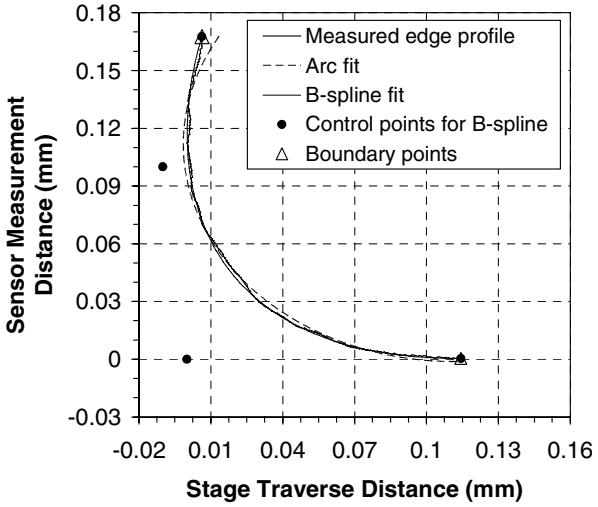

FIGURE 9. MEASURED EDGE PROFILE DATA, LEAST SQUARE FIT, CIRCULAR ARC AND OPTIMIZED B-SPLINE CURVE FIT.

CONCLUSIONS

This research studied AJM for edge generation, conoscopy laser for edge profile measurement, and B-spline and curve fitting methods for better representations of the developed edge. Based on the results of the AJM Inconel 718 samples, radii below 0.14 mm can be developed on 90º edge. For extended blasting times, the edge radius did not change

much, but the collateral damage increased rapidly. The nozzle angle and stand off distance to the edge have proven to be important in reducing the collateral damage to the edge. For the distances and angles studied, the radius size did not appear to be dependent on distance and angle. However, the collateral damage depth increased and the distance of the damage decreased as *l* was decreased or as α was increased. Therefore, if small amounts of damage on adjacent surfaces are acceptable, it is best to place the nozzle away from the sample and at a specific angle. Also, a B-spline was demonstrated to have a better fit than the arc. However, how to accurately describe and quantify the edge profile is still a challenging research topic.

This study indicates that a new technical challenge is in the generation of large edge radiuses. AJM has limited capability to generate large edge radius. Mechanical methods, such as brushing or grinding, with flexible supports are candidate processes to create edges with large radius.

ACKNOWLEDGMENTS

The authors would like to thank the sponsorship of General Electric Aviation and the donation of nozzles and media from Comco, Inc.

REFERENCES

Balasubramaniam, R., J. Krishnan, and N. Ramakrishnan (1999). "An Experimental Study on the Abrasive Jet Deburring of Cross-Drilled Holes." *Journal of Materials Processing Technology*, Vol. 91, pp. 178-182.

Balasubramaniam, R., J. Krishnan, and N. Ramakrishnan (2000). "An Empirical Study on the Generation of an Edge Radius in Abrasive Jet External Deburring (AJED)." *Journal of Materials Processing Technology*, Vol. 99, pp. 49-53.

Canby, J. (2003). "Microabrasive Blasting 101." *Manufacturing Engineering*, Vol. 131, No. 5, pp. 79-90.

Cousens, A.K. and I.M Hutchings (1983). "Influence of Erodent Particle Shape on the Erosion of Mild Steel." Proceedings 6th International Conference on Erosion by Liquid and Solid Impact. Cambridge, UK, Sept. 5-8, 1983, pp. 41.1-41.8.

Gillespie, L.K. (1999). *Deburring and Edge Finishing Handbook*. Dearborn, MI: Society of Manufacturing Engineers.

Lemaster, R.L., A. Shih and Z. Yu (2005). "Blasting and Erosion Wear of Wood Using Sodium Bicarbonate and Plastic Media." *Forest Products Journal*, Vol. 55, No. 5, pp. 59-64.

Morrison, C.T., R.O. Scattergood, and J.L. Routbort (1986). "Erosion of 304 Stainless Steel." *Wear*, Vol. 111, pp. 1-13.

Park, D-S., M-W. Cho, H. Lee, and W-S. Cho (2004). "Micro-grooving of Glass Using Micro Abrasive Jet Machining." *Journal of Materials Processing Technology*, Vol. 146, pp. 234-240.

Qu, J., A. Shih, R.O. Scattergood, and J. Luo (2005). "Abrasive Micro-blasting to Improve Surface Integrity of Electrical Discharge Machined WC-Co Composite." *Journal of Materials Processing Technology*, Vol. 166, pp. 440-448.

Shaffer, W.R. (1999). "Cutting Tool Edge Preparation." SME Technical Paper No. MR99-235, pp. 1-8.

Shewmon, P.G. (1981). "Particle Size Threshold in the Erosion of Metals." *Wear*, Vol. 68, No. 2, pp. 253-258.

Slikkerveer, P.J., P.C.P. Bouten, and F.C.M. de Haas (2000). "High Quality Mechanical Etching of Brittle Materials by Powder Blasting." *Sensors and Actuators*, Vol. 85, pp. 296–303

Tilly, G.P. (1969). "Erosion Caused by Airborne Particles." *Wear,* Vol. 14, pp. 63-79.

Weightman, H.G. (1970). "Apparatus for Dispensing Powder Such as Abrasive Powder." U.S. Patent 3,638,839 filed July 18, 1969, and issued February 1, 1970.

Williams, J.A. (1994). *Engineering Tribology*. New York: Oxford University Press, p. 488.